Desalination and Water Treatment
www.deswater.com
32 (2011) 214–225
August
1944-3994 / 1944-3986 © 2011 Desalination Publications. All rights reserved.
doi: 10.5004/dwt.2011.2701

In-situ monitoring of polysulfone membrane formation via immersion precipitation using an ultrasonic through-transmission technique

Ying Cai, Jianxin Li*, Xiuwei Zhang, Yuzhong Zhang

State Key Laboratory of Hollow Fiber Membrane Materials and Processes, School of Materials Science & Engineering, Tianjin Polytechnic University,
Tianjin 300160, PR China
Tel. +86 (22) 2452 8072; Fax +86 (22) 2452 8055; email: jxli@tjpu.edu.cn, jxli0288@yahoo.com.cn

Received 12 July 2010; Accepted in revised form 14 December 2010

ABSTRACT

An ultrasonic through-transmission technique as a non-invasive technique was developed to monitor the formation process of asymmetric polysulfone (PSF) membrane via immersion precipitation. The effect of polymer content in the casting solution in water/1-methyl-2-pyrrolidinone (NMP)/PSF and ethanol (EtOH)/NMP/PSF systems on the membrane morphology were investigated. Results showed that the systematic movement of ultrasonic signals in the arrival time observed during the membrane formation is associated with the changes of sound velocity in the media. The shift of ultrasonic signals in the arrival time decreased with an increase in the PSF concentration in both water and EtOH coagulations. The arrival time of ultrasonic signals kept stable at the initial time of membrane formation and then gradually shifted with the membrane formation when using water as a coagulation agent. It is relevant to the formation of the dense skin layer and finger-like macrovoids as well as the out-diffusion of NMP from the bottom surface of the casting solution. The systematic shift of ultrasonic signals forward along transmission direction of the sound wave in time-domain with the membrane formation time using EtOH as a coagulation agent is correlated with the formation of the porous surface and sponge-like structure. It is the reason because the double diffusion between EtOH and NMP leaded to liquid–liquid phase separation and the shrinkage in the lateral layer, mainly dominated by the penetration of EtOH from the coagulation to the casting solution. The SEM and AFM observation of membrane morphology corroborated ultrasonic measurements.

Keywords: Ultrasonic through-transmission technique; Immersion precipitation; Polysulfone; Microporous membrane; Mass transfer rate

1. Introduction

The majority of commercial polymeric membranes has been fabricated by immersion precipitation [1,2]. To gain a clear understanding of the membrane formation mechanism, a number of in-situ and non-destructive techniques have been developed to monitor the phase separation process [3,4]. The most common approach is the light transmission [3,4]. Using the light method, a very important delay time between immersion and demixing can be quantified. Under rapid demixing conditions the membranes can be expected to have a very thin top layer and a sublayer with many macrovoids. In the case of membranes obtained by delayed demixing, the

* Corresponding author.

Presented at the Third International Conference on Challenges in Environmental Science & Engineering, CESE-2010
26 September – 1 October 2010, The Sebel, Cairns, Queensland, Australia

top layer will be very dense and thick [2]. McHugh and Tsay [5] developed laser techniques to monitor the phase separation process. They used the refraction of laser light by refractive index gradients in solution to monitor the diffusion front and the reflected light for the detection of the motion of the precipitation front.

Other studies involved detection of the growth of the phase-separated region using optical microscopy [6–9]. Koenhen et al. [7] used an optical microscope to observe phase separation phenomena during the formation of asymmetric membranes. They found that macrovoid growth and movement of the gel front could be followed as a function of time. They also investigated the influence of the polymer concentration on the growth rate of the precipitation front. Results showed that the growth rate decreased with increasing polymer concentration. The growth rates of both macrovoids and the gel front were found to be a function of the square root of time. Qin et al. [8,9] reported on the use of an online optical microscope–CCD camera experimental system to study the formation kinetics of a poly(phthalazine ether sulfone ketone) membrane via phase inversion during membrane formation. It was found that a single linear correlation between the square value of the movement of the precipitation front and gelation time exists for the whole gelation process.

Furthermore, Kim et al. [10] described micro Raman spectroscopy as a non-invasive technique for the in-situ study of asymmetric membrane formation and kinetic behavior via phase inversion. They revealed that changes in composition with time were successfully measured on the gelation bath side as well as inside the precipitated phase for the polysulfone/1-methyl-2-pyrrolidinone (solvent)/ethanol (nonsolvent) system.

Meanwhile, ultrasonic technique as an in-situ, non-invasive and real-time approach has been extensively used to measure membrane fouling and cleaning in different module configurations, such as flat-sheet [11–13], tubular [14] and hollow fiber [15]. Mairal et al. [11] used the ultrasonic time-domain reflectometry (UTDR) technique for the real-time characterization of calcium sulfate fouling of flat-sheet reverse osmosis (RO) membranes. The results showed a good correspondence between the declines in the ultrasonic signal amplitudes and the development of a fouling layer. Li et al. [12,13], used the UTDR technique for the real-time investigation of organic and inorganic fouling and the cleaning of ultrafiltration (UF) and RO membranes. Further, the UTDR technique was also used to monitor protein fouling on tubular UF membranes [14]. Recently, Xu et al. [15] developed an extension of UTDR for the real-time measurement of particle deposition in a single hollow fiber membrane. Results showed that the UTDR technique could distinguish and recognize the acoustic response signals from the various curved surfaces of the housing holder and the hollow fiber within a single hollow fiber membrane module. The systematic changes of acoustic responses from the inside surfaces of a hollow fiber in the time- and amplitude-domain as a function of the operating time were observed during the fouling experiments. UTDR has also been used to measurement the thickness changes of polymeric films [16]. According to this study, the results were in excellent agreement with a maximum error of less than Earlier studies carried out by the members of our former and present research groups generally focused on the development and application of the ultrasonic technique for the non-invasive monitoring of fouling and cleaning in membrane separations. The main objective of the present study is to develop an ultrasonic through-transmission technique for the real-time monitoring of membrane formation via phase inversion so as to provide a new method to reveal the relationship between the phase inversion rate and membrane morphology and to illustrate the mechanism of polymeric membrane formation. The effects of different polymer concentrations and coagulation baths on the membrane morphology were investigated.

2. Experimental

2.1. Materials

Polysulfone (PSF) (Udel 3500, Mw = 50,000 Da) was used as membrane material. 1-methyl-2-pyrrolidinone (NMP) (Yingdaxigui Co. Ltd., Tianjin, China, analytical reagent) was used as solvent. The nonsolvents for PSF were deionized water and EtOH (Tianjin No.1 Chemical Reagent Factory, Tianjin, China, analytical reagent). All materials were used as received.

2.2. Membrane preparation

Microporous membranes were prepared using the immersion precipitation method. Water/NMP/PSF and EtOH/NMP/PSF systems were used as casting solutions. A certain amount of PSF was dissolved in NMP to form a homogeneous solution at 70°C. The concentration of PSF casting solution used was 10, 15, 20, 25 and 30 wt%. The casting solution was kept at 25°C for 24 h and cast on a glass plate at a uniform thickness (ca. 300 μm). Then, the glass plate with casting solution was directly immersed into the nonsolvent bath to form a microporous membrane. Herein the glass plate and the coagulation bath were kept at the same temperature as the polymer solution (25.0 ± 0.1°C).

2.3. Ultrasonic through-transmission system and measurements

Ultrasonic measurements are based on the propagation of sound waves. The sound velocity (c) through a medium is a function of the mass density (ρ) and the elastic constants (impedance) of the medium [17,18]. A schematic representation of the experimental setup for the measurement of phase inversion rate during membrane

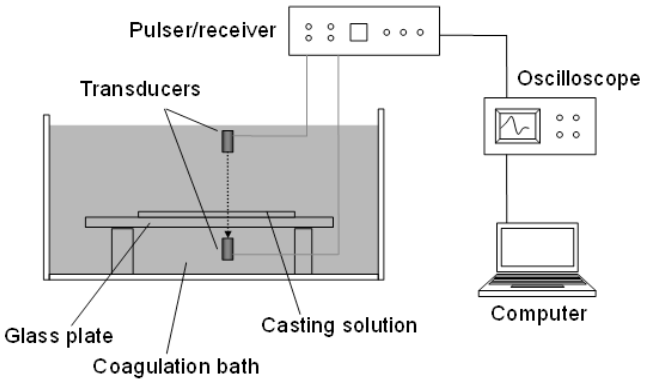

Fig. 1. Schematic diagram of the experimental setup used for the ultrasonic measurements.

formation is shown in Fig. 1. The ultrasonic measurement system consisted of two 10 MHz ultrasonic transducers (Panametrics V111), a pulser-receiver (Panametrics 5058PR) and a 350 MHz digital oscilloscope (Agilent 54641A) with sweep speeds from 1 to 50 ns per division and 2 mV per division sensitivity. In here, the frequency of ultrasonic transducer used is high enough to avoid the heat and cavitation effects. An oscilloscope was connected to the pulser-receiver to capture and display the data on its front panel. Each set of ultrasonic data generated consisted of 2000 data points. A glass plate with the casting solution was placed between the two transducers. One transducer was used as a transmitter and the other as a receiver. The ultrasonic wave pulses emitted from one transducer then propagated through the coagulation solution, casting solution, glass plate, to the receiving transducer. As the pulses encounter the receiver transducer they will be represented as through-transmission signal spectra in amplitude versus arrival time. The time required (Δt) for sound waves to travel from the emitter transducer to the receiver is a function of the path length (ΔS) and velocity (c), as given by Eq. (1)

$$\Delta t = \frac{\Delta S}{c} \tag{1}$$

Herein, the distance between the two transducers was 20 mm. Δt is related to the membrane formation process, i.e. the NMP concentration in the casting solution water/NMP/PSF or EtOH/NMP/PSF system and coagulation solution bath would change with the formation of microporous membrane as a result of the diffusion between nonsolvent and solvent (the time required at initial time can be calculated using the ultrasonic velocities), leading to the changes in the sound velocity or arrival time through a medium. Thus, the ultrasonic through-transmission measurements were performed in order to quantify the rate of membrane formation and to explore the relationship between the phase inversion rate and membrane morphology.

2.4. Membrane characterization

The PSF membranes obtained were subjected to morphological analysis using a scanning electron microscope (SEM) (JSM-6700F, JEOL, Japan). The membrane samples were freeze-dried, then frozen in liquid nitrogen and fractured to expose the cross-sectional areas. The dried samples were coated with gold, and viewed by SEM at 20 kV. Atomic force microscope (5500AFM, Agilent) was used to investigate top surface morphologies of the freeze-dried PSF membranes.

3. Results and discussion

3.1. Membrane preparation by water/NMP/PSF system

As mentioned above, water/NMP/PSF system was selected to prepare PSF membranes. When the casting solution on the glass plate was immersed into the coagulation bath, NMP diffused into the coagulation bath from the nascent membranes whereas water diffused into the casting solution [19]. As the nonsolvent merged into the precipitation phase, the casting solution changed from viscous solution to gel, and then to microporous membrane [20]. Fig. 2 shows the ultrasonic spectra corresponding to the amplitude of through-transmission signal (Peak A) in volts (V) vs. arrival time in seconds (s) during the membrane formation in water/NMP/PSF system (10 wt% PSF). The shift of acoustic signals in the time-domain with the membrane formation time from 2 s to 60 s was observed. The double diffusion between solvent (NMP) from casting solution to the coagulation bath (water) and nonsolvent (water) to casting solution resulted in the changes of the NMP concentration in both coagulation bath and the precipitation phase during the membrane formation. Hence, there would be two aspects contributing to the shift of ultrasonic signals: (1) mass transfer between water and NMP in both the coagulation

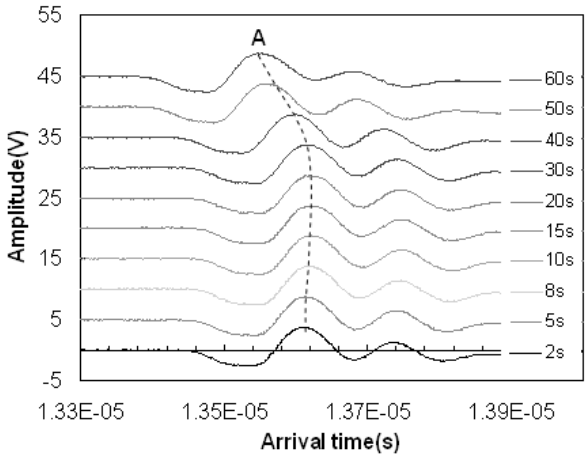

Fig. 2. Ultrasonic spectra obtained during membrane formation (10 wt% PSF) in water coagulation bath.

bath and the precipitation phase; (2) heat transfer due to the mixing heat between NMP and water [21]. Actually, though all the temperatures were kept the same and constant at the beginning, the mass transfer process was accompanied by a heat transfer during the immersion precipitation. The effect of heat transfer caused by the heat of mixing [22] is presently being investigated using an UTDR technique and will be reported in our future work. Here the immersion precipitation is regarded as an isothermal process [2]. Consequently, the shift of ultrasonic signals in the time-domain obtained is related to the ultrasonic velocities through the media or the changes in the density of the media as a result of the double diffusion between NMP and water.

An attempt to ascertain the relationship between the sound velocity and the double diffusion requires information about the relationship between the sound velocity and the concentration of a NMP/water mixture. The sound velocities in a NMP/water mixture can be obtained by ultrasonic measurements. Herein, the arrival time of the through-transmission ultrasonic signal in a NMP/water mixture (with different NMP concentrations) was measured in a cell with dimensions 50 mm × 50 mm × 100 mm. The sound velocity in the NMP/water mixture could be calculated by Eq. (1) as shown in Fig. 3. The sound velocity of the NMP/water mixture increased from 1490 to 1745 m/s with an increase in the NMP concentration from 0 to 60 wt%, and then decreased to 1546 m/s with an increase in the NMP concentration from 60 to 100 wt%. It means that there is an increase in the sound velocity once the NMP mixes with water. As a consequence, the shift of the acoustic signals in the time-domain observed in Fig. 2 was associated with the diffusion between solvent (NMP) in the casting solution and nonsolvent (water) in the coagulation bath. The initial NMP concentration was 90 wt% in the precipitation phase. The NMP concentration in the casting solution would decrease with the diffusion of water into the precipitation phase, resulting in the increased velocity. Simultaneously, the sound velocity in the coagulation solution would increase with the increase of NMP concentration in the coagulation solution as the diffusion of NMP into water. The more NMP diffused into water, the higher sound velocity the coagulation has. Changes in the sound velocity of the NMP and water mixture are relevant to the changes in the density of the mixture.

To illustrate the shift of ultrasonic signals more clearly, the shift rate ($\Delta t'$) of Peak A in arrival time obtained with different concentrations of the PSF casting solution during the membrane formation is summarized as shown in Fig. 4. Note: $\Delta t'$ is the difference in arrive time of Peak A at the initial time and a certain time of the membrane formation. Based on the acoustic signal from the glass plate, the arrival time of Peak A at the initial time was obtained by the calculation of the transmission time of the sound through the casting solution on the glass plate

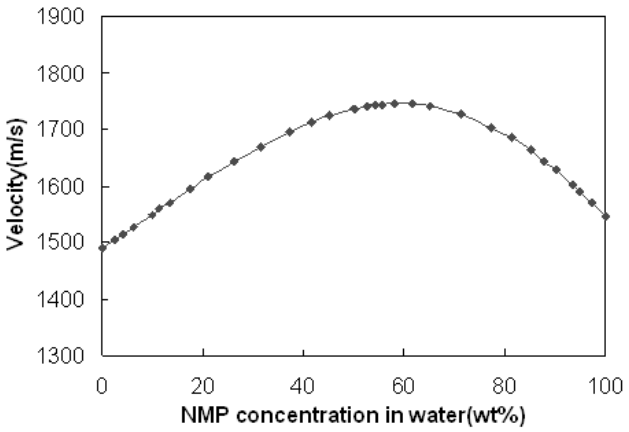

Fig. 3. NMP concentration in water vs. sound velocity.

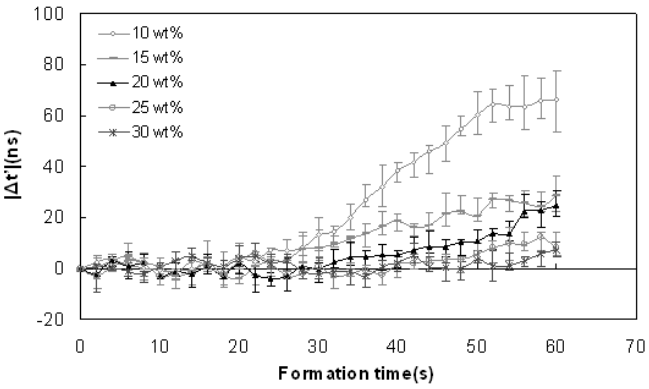

Fig. 4. Movements of ultrasonic signals in time-domain during the membrane formation in water coagulation bath.

according to the thickness and sound velocity of the casting solution. The velocities in the casting solutions with 10, 15, 20, 25 and 30 wt% PSF were 1563, 1570, 1576, 1585 and 1593 m/s. It can be seen from Fig. 4 that the shift of the ultrasonic signals in the time-domain increased with the membrane formation time. Note: the $\Delta t'$ values are negative. It means that the sound velocity through the media (the coagulation and casting solutions) increased and the arrival time of Peak A shortened (or Peak A shifted back) with the membrane formation as a consequence of the double diffusions between NMP and water. That is to say, the shift rate of the ultrasonic signal in the arrival time can be used to quantify the rate of mass transfer.

It can also be seen from Fig. 4 that the $\Delta t'$ absolute values in time-domain shift decreased with the increase of PSF concentrations. The $\Delta t'$ absolute value was nearly 80 ns for the low PSF concentration (10 wt% PSF), whereas it was only 16 ns for the high PSF concentration (30 wt% PSF) at 60 s of immersion. The diffusion rate at the lower PSF concentration was faster than that at the higher concentration owning to a low viscosity. The fast diffusion rate leads to a rapid increase in ultrasonic velocity. Hence, an increase in the shift rate of ultrasonic signals

in time-domain was be observed. The phase separation stage after gelation leads to the levitation of the membrane from the glass plate. It is found from Fig. 4 that the levitation time obtained is approximately 25 s for 10 wt % and 15 wt% PSF systems, 30 s for 20 wt % PSF and 40 s for 25-30 wt % PSF.

In order to corroborate the acoustic observation, the membrane samples obtained were subjected to SEM and AFM analyses so as to demonstrate the relationship between the concentration of the precursor polymer solution and the membrane morphology as shown in Figs. 5 and 6. Fig. 5 shows the micrographs of the membranes obtained at different polymer concentrations. All the membranes exhibited a typical asymmetric structure, consisting of a dense skin and a thick porous support. However, large macrovoids existed in part of the cross-section of the membrane obtained at lower polymer concentrations (Figs. 5a and b). The dense skin was very thin. The overall structure does not provide sufficient self-supporting mechanical properties. This is because a fast diffusion of NMP into the water bath resulted in the quick formation of very thin dense top layer at a low PSF concentration. It is noted that the rapid shift rate of the ultrasonic signals obtained was observed at the low PSF concentration. The formation of dense top layer corresponded to a macrovoid sublayer (Fig. 5a).

It also can be seen from Fig. 5 that the macrovoids gradually diminished and finger-like voids in the central part of membrane cross-section appeared with the increasing of PSF concentration. Both macrovoids and finger-like voids can be observed in the membranes obtained by 20 wt% PSF as shown in Fig. 5b. A significant amount of finger-like voids traversing through the whole membrane was obtained in Fig. 5c when the PSF concentration in the casting solution increased to 25 wt%. Furthermore, as the polymer concentration increased to 30 wt%, a very low shift rate was observed in ultrasonic signals. The shift rate or/and levitation time of the ultrasonic signals was the minimum. It corresponds to the appearance of a sponge-like structure as shown in Fig. 5e. A low polymer concentration in the casting solution contributed to a high mass transfer rate, leading to the formation of a finger structure, whereas a high polymer concentration resulted in the appearance of sponge-structure membranes. It implies that the mass transfer rate of solvent and nonsolvent strongly affected the membrane morphology. The mass transfer rate of membranes with finger structure is much faster than that with the sponge structuAn interesting phenomenon is that $\Delta t'$ absolute value in the arrival time shift kept stable at about 0 ns at the initial period of membrane formation (0–20 s) (Fig. 4). It can be explained by using the solubility parameters between nonsolvent (water) and solvent (NMP) as well as between a polymer (PSF) and a nonsolvent (water) during the membrane formation process [23–26]. On the moment the casting solution and coagulation solution (water) contacted, NMP in the casting solution diffused rapidly into the water coagulation bath as a result of a strong interaction between the water and NMP molecules (Table 1). On the other hand, relatively little water penetrated into the casting solution due to the low solubility of water in the PSF (Table 2). Consequently, the PSF molecules at the interface aggregated rapidly to form a dense skin at the surface. At this point, it can be confirmed from AFM images of the PSF membrane surfaces in Fig. 6. AFM images revealed that the roughness of the top surfaces of the membranes declined from 8.3 nm to 1.4 nm with the increase of PSF concentration from 10 wt% to 30 wt%. It implies that the skin layer of the membrane obtained becomes smooth and dense with the increase of PSF concentration. This dense skin hindered the further diffusion of NMP from underlying layer through the dense layer to the water bath and the permeation of water to the casting solution. As a result, the composition below the skin layer does not change so fast. Hence the solvation energy also does not change rapidly and the underlying solution is within the initial stable homogeneous region. Since the contact between water and NMP was favored over that of NMP and PSF, the PSF molecules were clustered together to exclude as much NMP as possible from within their domains. Thus, finger-like cavities were clearly observed in the membrane (Fig. 5).

Meanwhile, the formation process for finger-structured membranes is more complex and the stress relaxation in the precipitated polymer may play an important role [27]. The homogeneous layer easily ruptures when the shrinkage stress in the solid polymer skin could not be relieved by creep relaxation of the polymer. Once a finger initiated, shrinkage of the polymer caused it to propagate by draining the freshly precipitated polymer. The exchange of solvent and precipitant within a finger was much faster than that through the uncracked skin. Thus the precipitation front moved much faster within a finger than in the casting solution bypassed between fingers. Finally, the NMP in the sublayer of casting solution would diffuse out through the bottom surface to the water coagulation bath with the gradual solidification of upper part of the casting solution, although the bottom skin might form as a result of the adhesion of the casting solution to the glass plate, preventing the last polymer fluid at the bottom of the finger from moving to the sides of finger (this fluid polymer thus solidifies in place sealing off the finger). SEM analysis obtained confirms the above observations as shown Fig. 5. It can be seen from Fig. 5 that there were many pores on the bottom surface of membranes obtained using water as a coagulation agent. A high NMP concentration tends to form the membranes with more pores on the bottom surface.

To sum up, according to the observations of the ultrasonic measurements and membrane structure, the formation process of microporous membrane for water/NMP/PSF system deduced included four steps as illus-

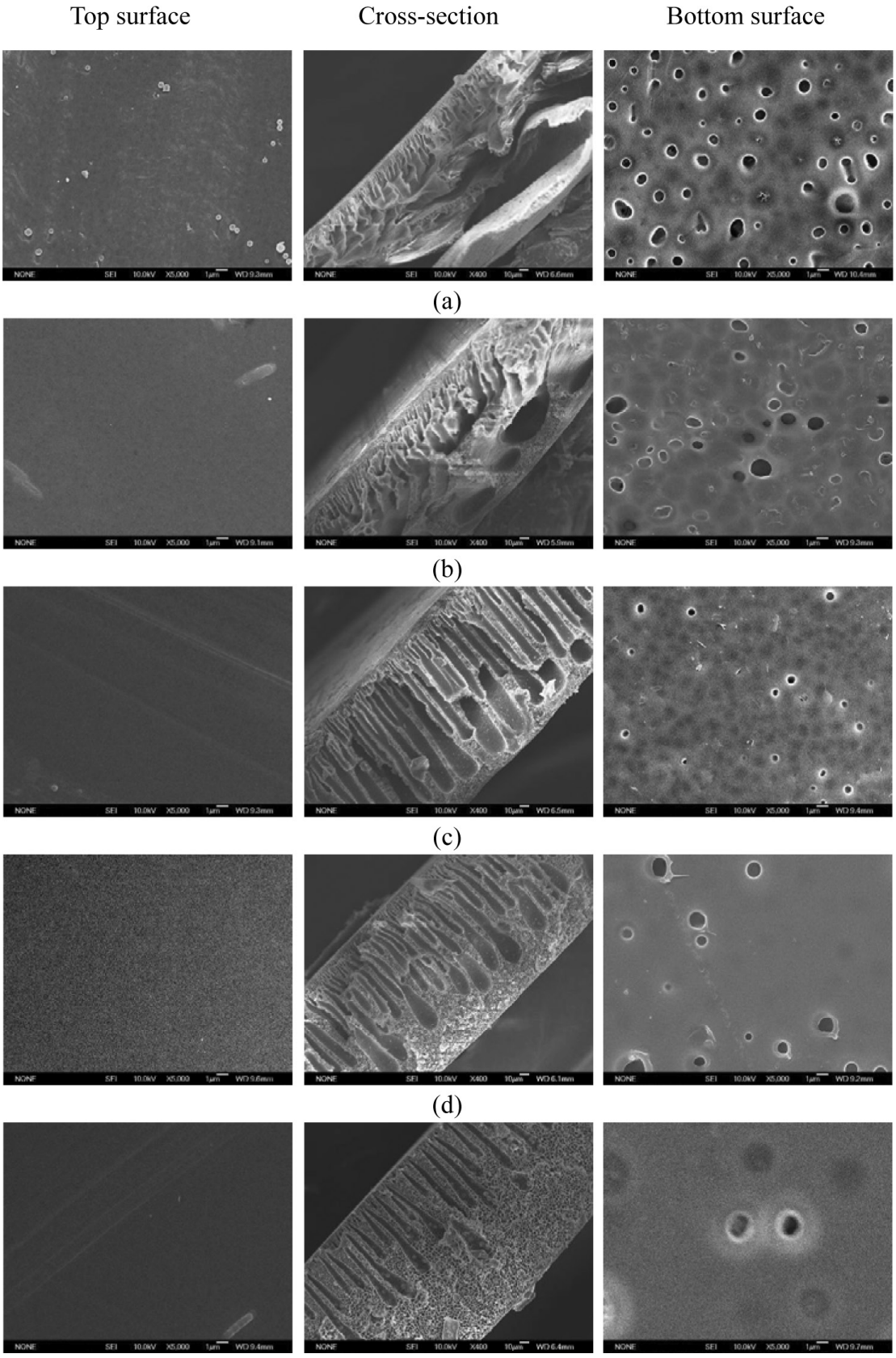

Fig. 5. SEM images of the membranes with different PSF concentrations obtained in a water coagulation bath: (a) 10 wt%; (b) 15 wt%; (c) 20 wt%; (d) 25 wt%; (e) 30 wt%.

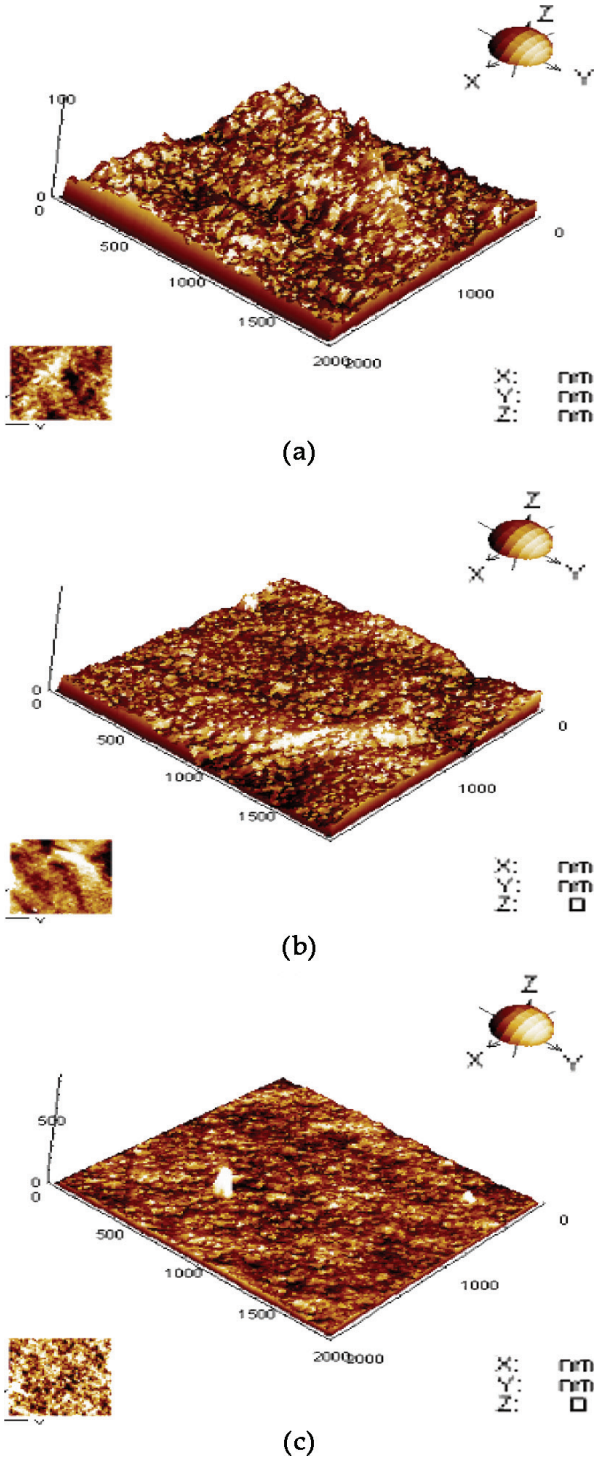

Fig. 6. AFM images of the top surfaces of the membranes with different PSF concentrations obtained in a water coagulation bath: (a) 10 wt% PSF, RMS: 8.3 nm; (b) 20 wt% PSF, RMS: 5.5 nm; (c) 30 wt% PSF, RMS: 1.4 nm.

trated in Fig. 7: (1) out-diffusion of NMP from the top surface of the casting solution and dense layer formation (2) solidification of the upper part of the casting solution

Table 1
Solubility parameters δ and solubility parameter disparity |Δδ| of substance and NMP

Substance	δd (MPa)1/2	δp (MPa)1/2	δh (MPa)1/2	δsp (MPa)1/2	$\lvert\Delta\delta\rvert$ (MPa)1/2
Water	15.5	16.0	42.4	47.9	35.5
EtOH	15.8	8.8	19.4	26.6	12.9
NMP	18.0	12.3	7.2	22.9	

(liquid–solid phase separation) and finger-structure formation, (3) formation of the sublayer and out-diffusion of NMP from the bottom surface of the casting solution, (4) formation and levitation of the membrane.

The morphology observations of the membranes corroborated the results of ultrasonic measurements. In order to consolidate the above observations, the membrane formation process using EtOH as coagulation was further monitored by the ultrasonic technique so as to investigate its adaptability to different coagulation solutions.

3.2. Membrane preparation by EtOH/NMP/PSF system

The ultrasonic spectra corresponding to the through-transmission signals during the membrane formation of 10 wt% PSF in EtOH coagulation was summarized in Fig. 8. Different from the formation process in water coagulation, the ultrasonic signals shifted forward along transmission direction of the sound wave in time-domain with the membrane formation time (Fig. 8). It suggests that the sound velocities through the media of the coagulation and casting solution decreased during the membrane formation. It can be explained by the relationship between the sound velocity and the concentration of a NMP/EtOH mixture as shown in Fig. 9.

Fig. 9 shows that the sound velocities in EtOH and NMP are 1138 m/s and 1546 m/s. A quasi linear relationship between the sound velocity and the NMP concentration in EtOH existed. The initial NMP concentration was 90 wt% in the precipitation phase. The concentration of NMP in precipitation phase decreased and the concentration of EtOH increased with the formation time as a result of the diffusions between NMP and EtOH, i.e. EtOH from the coagulation to the casting solution and NMP from the casting solution to the coagulation. Both led to the decreased velocity in precipitation phase. On the other hand, the sound velocity in the coagulation bath increased with an increase of the NMP concentration in the coagulation bath from 0 wt% to approximately 2 wt% (once all the NMP in the precipitation phase diffuse out into the coagulation bath). So the shifts of ultrasonic signals in time-domain resulted from the changes of the sound velocity both in the coagulation bath and the casting solution. Obviously, the shift of ultrasonic signals

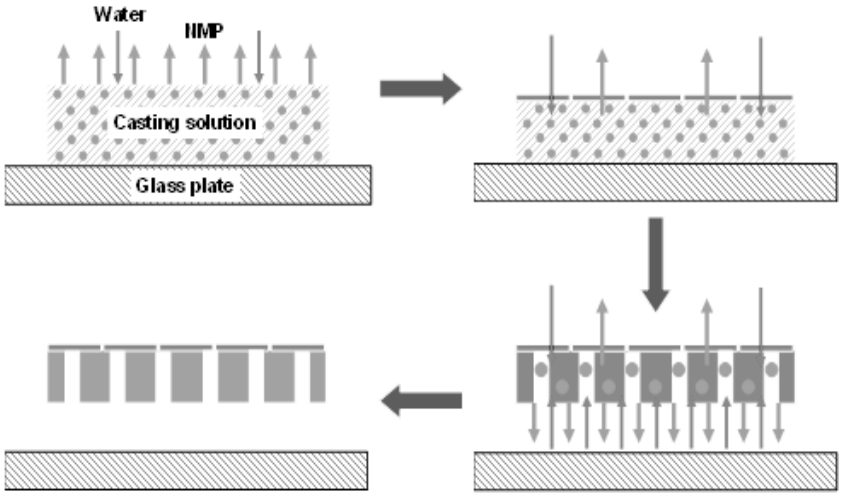

Fig. 7. PSF membrane formation steps using water as a coagulation: (1) out-diffusion of NMP and dense layer formation; (2) solidification of the upper part of the casting solution and finger-structure formation; (3) formation of the sublayer and out-diffusion of NMP from the bottom surface of the casting solution; (4) formation and levitation of the membrane.

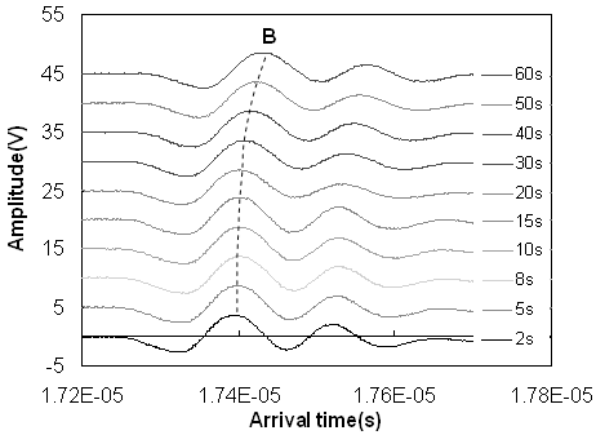

Fig. 8. Ultrasonic signal spectra during membrane formation (10 wt% PSF) in EtOH coagulation bath.

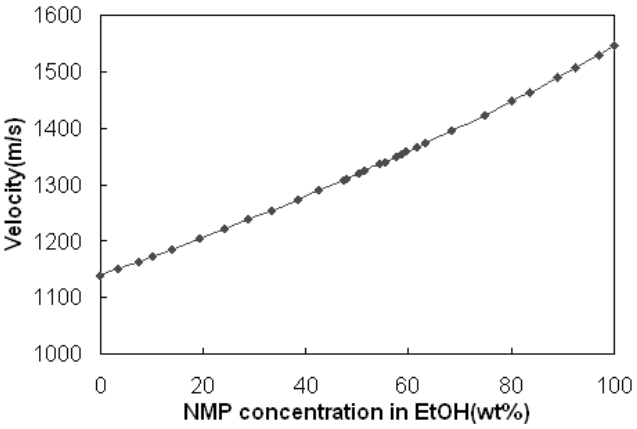

Fig. 9. NMP concentration in EtOH vs. sound velocity.

obtained in Fig. 8 was mainly controlled by the changes of the sound velocity in the casting solution, namely the penetration of EtOH from the coagulation to the casting solution. The shift rate ($\Delta t'$) of ultrasonic signal Peak B in arrival time during the membrane formation was illustrated in Fig. 10.

Fig. 10 indicates that the shift of the ultrasonic signal in time domain increased with the formation time. It also can be found from Fig. 10 that the shift rate of ultrasonic signal in time-domain decreased with the increase of PSF concentration in the casting solution due to a decrease in the concentration of NMP in the casting [10]. $\Delta t'$ obtained with the low PSF concentration (10 wt% PSF) was nearly 60 ns at 60 s of immersion, whereas the movement was only 15 ns at the high PSF concentration (30 wt% PSF). The shift rate of ultrasonic signals in time domain obtained with 30 wt% PSF was low and kept quite stable. Further, the levitation time of the membrane using EtOH as a coagulation agent is over 300 s, which is much longer than that using water.

After the membrane formation and the acoustic measurements, the membrane samples obtained were subjected to SEM analysis. Fig. 11 shows the cross-section micrographs of the microporous membranes precipitated in EtOH. The large macrovoids of the membrane in part of the cross-section can be observed in Fig. 11a, owing to a fast double diffusion between EtOH and NMP at a lower PSF solution (10 wt% PSF). In the same way, the membrane with both macrovoids and sponge-like voids obtained by 15 wt% PSF solution can be seen in Fig. 11b.

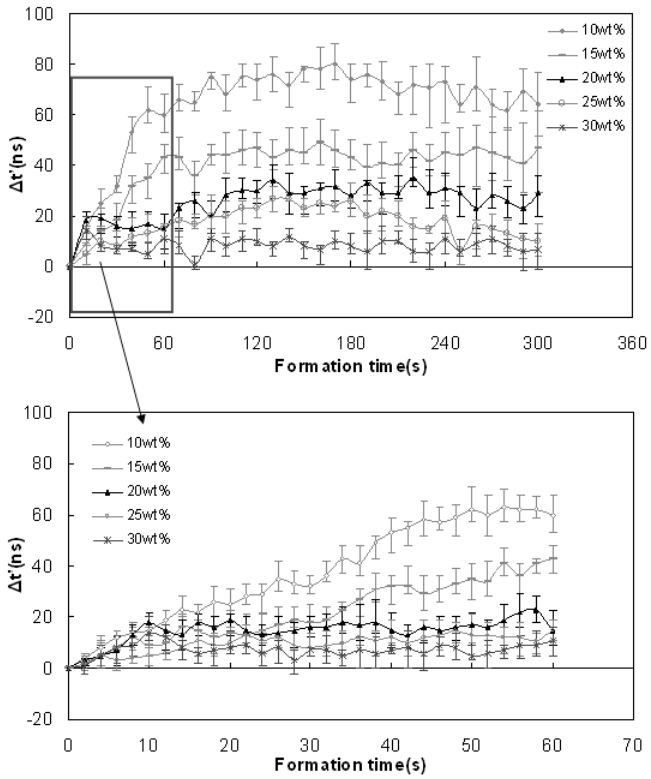

Fig. 10. Movements of ultrasonic signals in time-domain during the membrane formation in EtOH coagulation bath.

However, it is found from Fig. 11 that the macrovoid structure in the microporous membrane gradually diminished and sponge-like structure appeared with the increase of the PSF concentration in casting solution as a result of a gradual decrease in the mass transfer rate. When the PSF concentration increased to 20 wt%, the macrovoid diminished completely, and the membrane gradually exhibited a symmetric structure of sponge-like voids (Fig. 11c, 11d and 11e). The higher the polymer concentration of the precipitate phase is, the denser and thicker the developed membrane skin is, resulting in a low double diffusion rate during membrane formation. The morphological observations of the membranes therefore corroborated with the ultrasonic measurements.

For the EtOH/NMP/PSF system, the membrane with a loose, open sponge-like structure was obtained (Fig. 11). On the one hand, the solubility parameter disparity between EtOH and NMP is lower than that of water and NMP (see Table 1). NMP easily diffused out from the casting solution into the EtOH coagulation bath. On the other hand, the solubility of EtOH in PSF is higher than that of water (Table 2). The diffusion rate of EtOH into the casting solution was higher than that of water. In other words, the interactions between PSF molecules were not particularly strong and PSF molecules maintained the dispersed state. This is the reason that the surface of the casting solution adjacent to the nonsolvent (EtOH) does not precipitate rapidly and compactly. Consequently, the membrane with a porous surface formed (Fig. 11).

Further, the diffusion rate of NMP from the underlying solution was about the same as from the surface solution since the porous surface did not influence the diffusion rate. For EtOH to enter this region, it can easily diffuse through the upper porous surface to induce the liquid-liquid phase separation. In this way, the porous membrane with a sponge-like structure formed. In like manner, the NMP in the sublayer of casting solution would diffuse out through the bottom surface to the EtOH coagulation bath with the gradual solidification of upper part of the casting solution. Similarly, a high NMP concentration tends to form the membranes with more pores on the bottom surface. However, the number of pores on the bottom surface of the membrane obtained using EtOH as coagulation agent was fewer than that using water. This is because most of NMP in the casting solution diffused out from the top surface into the coagulation. Consequently, the gradual and systematic changes in the ultrasonic signals obtained during the membrane formation are in good agreement with the above SEM analyses.

In a word, according to the above observations, the formation process of microporous membrane in EtOH/NMP/PSF system deduced included four steps as shown in Fig. 12: (1) double diffusion of NMP from the casting solution into the coagulation bath and EtOH from the coagulation bath into the coagulation bath at the upper part of the casting solution; (2) double diffusion from the underlying solution into the surface solution (liquid–liquid phase separation) and solidification of the upper part of the casting solution; (3) solidification of the sublayer and out-diffusion of NMP from the bottom surface of the casting solution; (4) formation and levitation of the membrane (Fig. 12).

Equally, different diffusion behaviors and rates of solvent (NMP) from the casting solution into the coagulation bath and nonsolvent from the coagulation into the casting solution affect the shrinkage of the membrane. Fig. 13

Table 2
Solubility and interaction parameters χ of water and EtOH in the polymer PSF

Nonsolvent	Solubility (g nonslovent/100 g dry PSF)	Volume fraction of polymer	χ
Water	0.1	0.999	5.9
EtOH	2.3	0.96	2.5

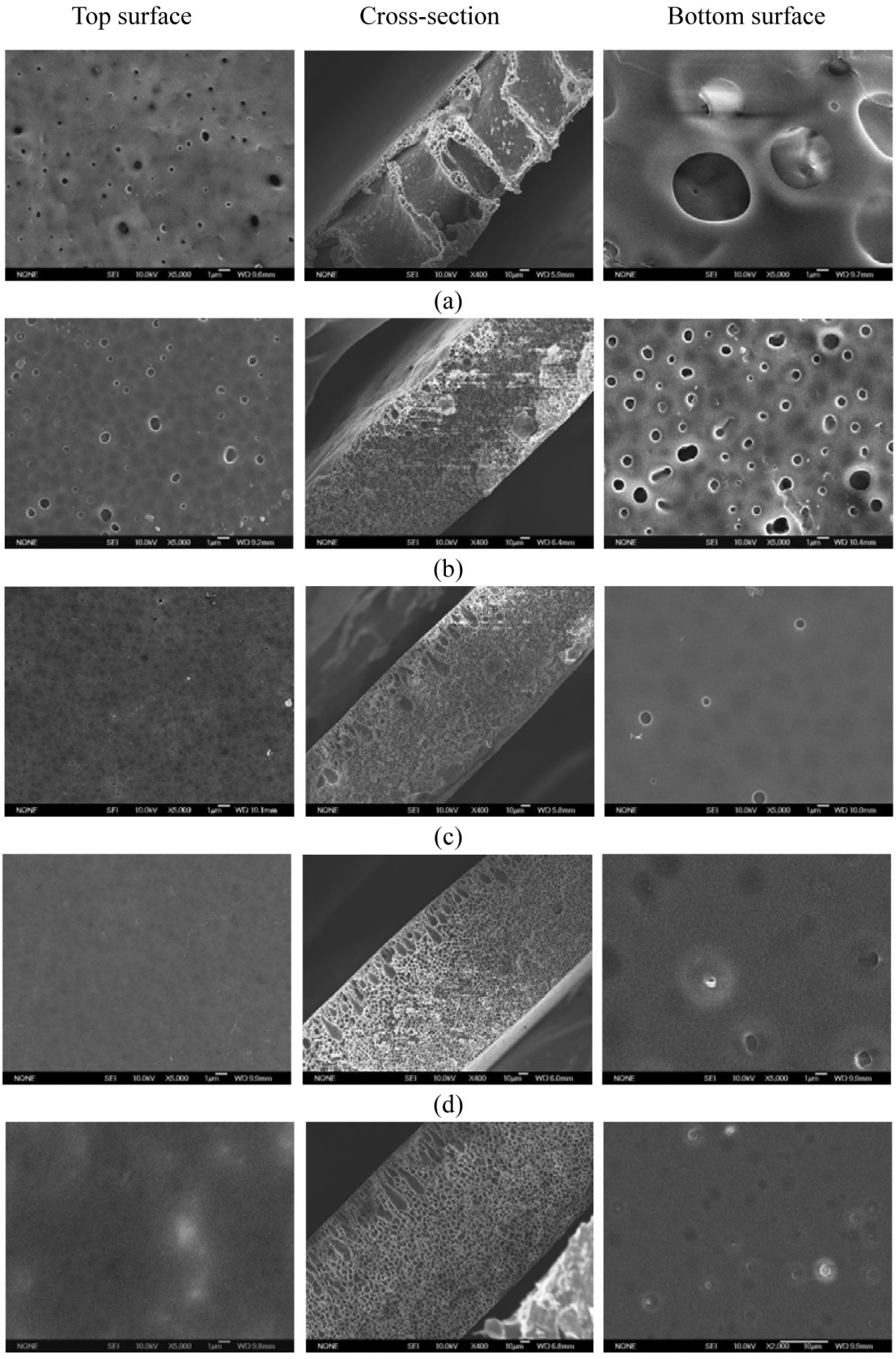

Fig. 11. SEM images of the membranes with different PSF concentrations obtained in an EtOH coagulation bath: (a) 10 wt%; (b) 15 wt%; (c) 20 wt%; (d) 25 wt%; (e) 30 wt%.

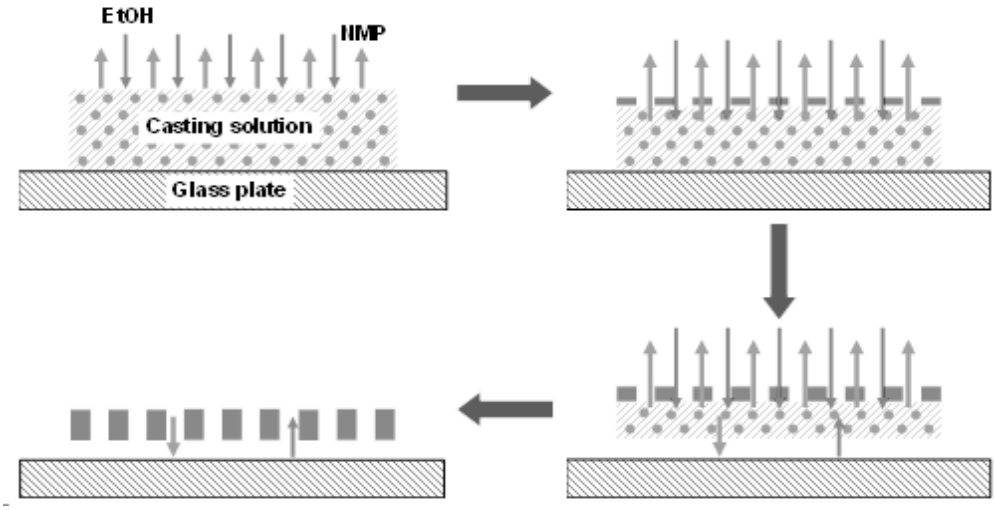

Fig. 12. PSF membrane formation steps using EtOH as a coagulation: (1) double diffusion at the upper part of the casting solution; (2) double diffusion from the underlying solution into the surface solution and solidification of the upper part of the casting solution; (3) solidification of the sublayer and out-diffusion of NMP from the bottom surface of the casting solution; (4) formation and levitation of the membrane.

demonstrates the thickness of PSF membranes obtained in water and EtOH coagulation baths, respectively. It can be seen from Fig. 13 that the PSF membranes obtained in the water coagulation bath were much thicker than those in the EtOH bath. For example, the thickness of the 10 wt% PSF membrane obtained in the water coagulation bath was about 190 μm, whereas the thickness of the same PSF concentration membrane obtained in the EtOH bath was only 150 μm. Note: the thickness of the casting solution is approximate 300 μm. The extent of shrinkage was strongly influenced by the ratio between nonsolvent in-flux and solvent out-flux from the polymer solution during membrane formation [28]. Compared with water as nonsolvent, EtOH was much easier to enter the casting solution than water. It would lead to the shrinkage in the lateral layer. In the case of shrinkage, each layer of the membrane obtained in the EtOH bath contributes to the total shrinkage [29]. At the same time, the solubility parameter disparity of EtOH and NMP was lower than that of water and NMP (see Table 1). It is speculated that NMP out-flux in EtOH as a coagulation agent was lower than that in water at the top-surface of the membrane. Thus the formation of the membrane with a porous skin would not hinder the further diffusion between NMP and EtOH. The diffusion rate of NMP from the underlying solution was almost the same as from the surface solution. The shift of ultrasonic obtained in time-domain gradually increased after immersion. Finally, all the membranes obtained in the EtOH coagulation bath were thinner than those in the water coagulation bath.

Based on the above observations of ultrasonic measurements, it is easy to know that changes of ultrasonic signals in the arrival time are associated with different mechanisms of membrane formation. The ultrasonic transmission technique is capable of distinguishing the different behaviors of PSF membrane formation between water and EtOH as nonsolvents or coagulations. In the meantime, different behaviors of membrane formation result in different membrane structures obtained.

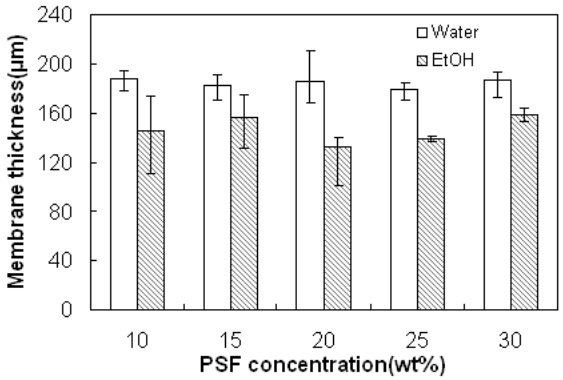

Fig. 13. Thickness of PSF membranes obtained in water and EtOH coagulation baths.

4. Conclusions

An ultrasonic through-transmission technique was successfully developed to in situ monitor the formation process of PSF membranes in both water/NMP/PSF and EtOH/NMP/PSF systems. The shift rate of ultrasonic

signals in the arrival time decreased with an increase in the PSF concentration in both water and EtOH coagulations. The formation of the membrane with the dense skin layer and finger-like macrovoids was related to the out-diffusion of NMP from the bottom surface of the casting solution using water as a coagulation agent. Furthermore, the formation of the membrane with the porous surface and sponge-like structure was attributed to double diffusion between EtOH and NMP, leading to liquid–liquid phase separation and the shrinkage in the lateral layer, mainly governed by the penetration of EtOH from the coagulation to the casting solution. The observation of membrane morphology corroborated ultrasonic measurements. Overall, the ultrasonic technique will provide a new approach for the mechanism study of polymeric membrane formation.

Acknowledgements

The authors gratefully acknowledge the National Natural Science Foundation of China (Nos. 20676100 and 20876115) and the SA/CHINA Agreement on Cooperation on Science and Technology (No. 2010DF51090) for their financial support. We appreciate the constructive suggestions from Prof. Ron D. Sanderson at University of Stellenbosch, South Africa.

References

[1] M. Mulder, Basic Principle of Membrane Technology, Dordrecht: Kluwer Academic Publishers, 1996.
[2] P. van de Witte, P.J. Dijkstra, J.W.A. van den Berg and J. Feijen, Phase separation processes in polymer solutions in relation to membrane formation, J. Membr. Sci., 117 (1996) 1–31.
[3] A.J. Reuvers, J.W.A. van den Berg and C.A. Smolders, Formation of membranes by means of immersion precipitation: Part I. A model to describe mass transfer during immersion precipitation, J. Membr. Sci., 34 (1987) 45–65.
[4] P. Radovanovic, S.W. Thiel and S. Hwang, Formation of asymmetric polysulfone membranes by immersion precipitation. Part I. Modelling mass transport during gelation, J. Membr. Sci., 65 (1992) 213–22A.J. Mchugh and C.S. Tsay, Dynamics of the phase inversion process, J. Appl. Polym. Sci., 46 (1992) 2011–2021.
[5] M.A. Frommer and D. Lancet, The mechanism of membrane formation: membrane structures and their relation to preparation conditions, in A.K. Londsdale and H.E. Podall, eds., Reverse Osmosis Membrane Research. New York, Plenum Press, 1972.
[6] D.M. Koenhen, M.H.V. Mulder and C.A. Smolders, Phase separation phenomena during the formation of asymmetric membranes, J. Appl. Polym. Sci., 21 (1977) 199–215.
[7] P. Qin, C. Chen, Y. Yun, Z. Chen, T. Shintani, X. Li, J. Li and B. Sun, Formation kinetics of a polyphthalazine ether sulfone ketone membrane via phase inversion, Desalination, 188 (2006) 229–237.
[8] P. Qin, C. Chen, B. Han, S. Takuji, J. Li and B. Sun, Preparation of poly(phthalazinone ether sulfone ketone) asymmetric ultrafiltration membrane: II. The gelation process, J. Membr. Sci., 268 (2006) 181–188.
[9] H.J. Kim, A.E. Fouda and K. Jonasson, In situ study on kinetic behavior during asymmetric membrane formation via phase inversion process using Raman spectroscopy, J. Appl. Polym. Sci., 75 (2000) 135–141.
[10] A.P. Mairal, A.R. Greenberg, W.B. Krantz and L.J. Bond, Real-time measurement of inorganic fouling of RO desalination membranes using ultrasonic time-domain reflectometry, J. Membr. Sci., 159 (1999) 185–196.
[11] J. Li, D.K. Hallbauer and R.D. Sanderson, Direct monitoring of membrane fouling and cleaning during ultrafiltration using a non-invasive ultrasonic technique, J. Membr. Sci., 215 (2003) 33–52.
[12] Y. Hou, Y. Gao, Y. Cai, X. Xu and J. Li, In-situ monitoring of inorganic and microbial synergistic fouling during nanofiltration by UTDR, Desal. Wat. Treat., 11 (2009) 15–22.
[13] J.-X. Li, R.D. Sanderson and G.Y. Chai, A focused ultrasonic sensor for in situ detection of protein fouling on tubular ultrafiltration membranes, Sens. Actuators B: Chem., 114 (2006) 182–191.
[14] X. Xu, J. Li, H. Li, Y. Cai, Y. Cao, B. He and Y. Zhang, Non-invasive monitoring of fouling in hollow fiber membrane via UTDR, J. Membr. Sci., 326 (2009) 103–110.
[15] W.F.C. Kools, S. Konagurthu, A.R. Greenberg, L.J. Bond, W.B. Krantz, T. Van Den Boomgaard and H. Strathmann, Use of ultrasonic time-domain reflectometry for real-time measurement of thickness changes during evaporative casting of polymeric films, J. Appl. Polym. Sci., 69 (1998) 2013–2019.
[16] J. Krautkramer and H. Krautkramer, Ultrasonic Testing of Materials, Berlin: Springer-Verlag, 1990.
[17] A.S. Birks, R.E. Green and P. Mclntire, Nondestructive Testing Handbook, Ultrasonic Testing, 2nd ed., USA, ASNT, 1991.
[18] T.H. Young, J.Y. Lai, W.M. You and L.P. Cheng, Equilibrium phase behavior of the membrane forming water-DMSO-EVAL copolymer system, J. Membr. Sci., 128 (1997) 55–65.
[19] W.E. Laque and C.E. Ronneberg, A study of the decarboxylation of trichloroacetic acid in solutions of water and dimethylsulfoxide, Ohio J. Sci., 70 (1970) 97–106.
[20] D.D. Macdonald, D. Dunay, G. Hanlon and J.B. Hune, Properties of the N-methyl-2-pyrrolidinone water system, Can. J. Chem. Eng., 49 (1971) 420–423.
[21] L. Chen and T. Young, Effect of nonsolvents on the mechanism of wet-casting membrane formation from EVAL copolymers, J. Membr. Sci., 59 (1991) 15–26.
[22] J. Brandrup and E.H. Immergut, Polymer Handbook, 3rd ed., Wiley, New York, 1989.
[23] J. Xu and Z. Xu, Poly(vinyl chloride) (PVC) hollow fiber ultrafiltration membranes prepared from PVC/additives/solvent, J. Membr. Sci., 208 (2002) 203–212.
[24] M.H.V. Mulder and C.A. Smolders, On the mechanism of separation of ethanol/water mixtures by pervaporation I. Calculations of concentration profiles, J. Membr. Sci., 17 (1984) 289–307.
[25] M.H.V. Mulder, T. Franken and C.A. Smolders, Preferential sorption versus preferential permeability in pervaporation, J. Membr. Sci., 22 (1985) 155–173.
[26] H. Strathmann and K. Kock, The formation mechanism of phase inversion membranes, Desalination, 21 (1977) 241–255.
[27] C. Stropnik, V. Musil and M. Brumen, Polymeric membrane formation by wet-phase separation; turbidity and shrinkage phenomena as evidence for the elementary processes, Polymer, 41 (2000) 9227–9237.
[28] M. Bikel, I.G.M. Pünt, R.G.H. Lammertink and M. Wessling, Shrinkage effects during polymer phase separation on microfabricated molds, J. Membr. Sci., 347 (2010) 141–149.